Impact of land use/land cover types on surface humidity in northern China in the early 21st century

JIN Junfang[1], YIN Shuyan[1*], YIN Hanmin[2]

[1] School of Geography and Tourism, Shaanxi Normal University, Xi'an 710119, China;
[2] Xinjiang Institute of Ecology and Geography, Chinese Academy of Sciences, Urumqi 830011, China

Abstract: In the context of global change, it is essential to promote the rational development and utilization of land resources, improve the quality of regional ecological environment, and promote the harmonious development of human and nature for the regional sustainability. We identified land use/land cover types in northern China from 2001 to 2018 with ENVI images and ArcGIS software. Meteorological data were selected from 292 stations in northern China, the potential evapotranspiration was calculated with the Penman–Monteith formula, and reanalysis humidity and observed humidity data were obtained. The reanalysis minus observation (RMO, i.e., the difference between reanalysis humidity and observed humidity) can effectively characterize the impact of different land use/land cover types (forestland, grassland, cultivated land, construction land, water body and unused land) on surface humidity in northern China in the early 21st century. The results showed that from 2001 to 2018, the area of forestland expanded (increasing by approximately 1.80×10^4 km^2), while that of unused land reduced (decreasing by approximately 5.15×10^4 km^2), and the regional ecological environment was improved. Consequently, land surface in most areas of northern China tended to be wetter. The contributions of land use/land cover types to surface humidity changes were related to the quality of the regional ecological environment. The contributions of the six land use/land cover types to surface humidity were the highest in northeastern region of northern China, with a better ecological environment, and the lowest in northwestern region, with a fragile ecological environment. Surface humidity was closely related to the variation in regional vegetation coverage; when the regional vegetation coverage with positive (negative) contributions expanded (reduced), the land surface became wetter. The positive contributions of forestland and water body to surface humidity were the greatest. Unused land and construction land were associated with the most serious negative contributions to surface humidity. Affected by the regional distribution pattern of vegetation, surface humidity in different seasons decreased from east to west in northern China. The seasonal variation in surface humidity was closely related to the growth of vegetation: surface humidity was the highest in summer, followed by autumn and spring, and the lowest in winter. According to the results, surface humidity is expected to increase in northeastern region of northern China, decrease in northern region, and likely increase in northwestern region.

Keywords: surface humidity; land use/land cover change; reanalysis minus observation; Penman–Monteith formula; climate change; northern China

Citation: JIN Junfang, YIN Shuyan, YIN Hanmin. 2022. Impact of land use/land cover types on surface humidity in northern China in the early 21st century. Journal of Arid Land, 14(7): 705–718. https://doi.org/10.1007/s40333-022-0055-3

1 Introduction

Land use/land cover change (LUCC) is the most direct signal of the impact of human activities on

*Corresponding author: YIN Shuyan (E-mail: yinshy@snnu.edu.cn)
Received 2021-11-05; revised 2022-06-13; accepted 2022-06-18

the natural ecosystems on the Earth's surface. As an important link between human socioeconomic activities and natural ecological processes, LUCC has become a hot topic in the study of global climate and environmental change (Sterling et al., 2012; Mooney et al., 2013; Liu et al., 2014; Tuffour-Mills et al., 2020; Zhang et al., 2020; Sun et al., 2021). Studies have shown that LUCC is closely related to the circulation of surface materials and life processes and that at least one third of the Earth's surface is directly affected by human activities in the processes of exploiting land resources and implementing land cover change (Shao and Zeng, 2012; Tian et al., 2012; IPCC, 2019). In addition, as a key process in terrestrial ecosystems, LUCC plays important roles in the material cycle and energy flow. It mainly affects biogeophysical processes such as surface albedo, soil fluxes and vegetation evapotranspiration. Additionally, land coverage is essential not only for the transfer of energy between the land and atmosphere but also in the maintenance and optimization of ecosystem services, and it is also regarded as an "indicator" in the study of global climate change (Braswell et al., 1997; Sun et al., 2000; Wang et al., 2012; Buitenwerf et al., 2015; Verbeeck and Kearsley, 2015; Wang et al., 2016; Fu et al., 2017; Gao et al., 2019).

Scholars worldwide mainly use two methods to study the climatic impact of LUCC. One method involves scenario simulations, which simulate the climatic factors assumed in specific scenarios by constructing a model and then predict the possibility of a certain impact of LUCC on a global scale (Lai et al., 2016; Lin et al., 2020). For example, Hurtt et al. (2011) reconstructed the interannual variation characteristics of global LUCC through a global land-use model and explored the response of LUCC to the global carbon cycle and climate change. Many scholars have also assessed the impact of LUCC on global climate through multiple climate models or interdisciplinary models (Oleson et al., 2008; Pitman et al., 2009; Li et al., 2017; Wang et al., 2021). The other method is sensitivity analysis, which mainly explores the regional climatic impact of LUCC in a local area over a short time through remote sensing image data integrated with sediment, fossil or tree ring data (Dumont et al., 2015; Fezzi et al., 2015; Weinert et al., 2016). Studies based on this method focused mainly on precipitation and temperature. For example, many scholars (Yang et al., 2009; Cao et al., 2010; Bian et al., 2019) have shown that LUCC has a far-reaching impact on regional climate, especially on precipitation and temperature, mainly by affecting the surface energy budget, the Bowen ratio and the distribution of precipitation among evapotranspiration, infiltration and runoff. Under the background of global climate change, regional surface humidity has a direct and significant impact on vegetation coverage. If only natural factors are considered, the regional vegetation coverage is high, resulting in high surface humidity, and vice versa; this relation has been previously validated. However, due to the close and complex relationship between the spheres of the Earth, different vegetation cover types may also influence the characteristics of regional climate (e.g., evaporation, transpiration and the water retention of roots, stems and leaves). Consequently, different impacts on regional surface humidity may also be observed. Therefore, in terms of the study of regional surface dry-wet conditions for long time series, the influence of LUCC on surface humidity cannot be ignored.

Northern China spans a vast area (4.76×10^6 km^2), accounting for approximately half of the whole country. The climate here shows obvious regional heterogeneity and transitional characteristics. Most of northern China is in the dry-wet transition zone, so the ecological environment is highly fragile. Therefore, northern China is sensitive to global climate change. On the basis of a comprehensive consideration of various climatic factors, we objectively explored the impact of LUCC on surface humidity and its regional heterogeneity in northern China to provide a theoretical basis for human beings to rationally develop and utilize land resources, protect the regional ecological environment, and promote the harmonious development of the regional social economy and ecological environment.

2 Data and methods

2.1 Study area

Located north of the Qinling-Huaihe Line, northern China covers a vast area with the longitude

and latitude ranges of 73°33′–135°05′E and 35°00′–53°33′N, respectively. According to regional differences, we divided the 15 provinces, autonomous regions and municipalities in northern China into three regions: northeastern region (Heilongjiang Province, Jilin Province and Liaoning Province), northern region (Inner Mongolia Autonomous Region, Beijing City, Tianjin City, Shanxi Province, Hebei Province, Shandong Province and Henan Province) and northwestern region (Shaanxi Province, Gansu Province, Ningxia Hui Autonomous Region, Qinghai Province and Xinjiang Uygur Autonomous Region). In addition, there are significant differences between regional dry and humid zones in climate and vegetation types, which can span four dry-wet zones (humid zone, semi-humid zone, semi-arid zone and arid zone) from east to west, and the corresponding vegetation types change from forestland to grassland and even desert. It can be said that northern China is a sensitive area of global climate change.

2.2 Surface humidity data and processing

The climate data used in this study were derived from the daily surface climate datasets provided by the China Meteorological Data Service Centre (http://data.cma.cn). By excluding sites with missing data, 292 meteorological stations with complete observation data from 1991 to 2018 in northern China were selected for a comparative study with land use data (Fig. 1). The main climatic elements included in this study were the daily average temperature, daily maximum temperature, daily minimum temperature, sunshine duration, 2-min mean wind speed, daily precipitation, average water vapour pressure and atmospheric relative humidity. For each of these variables, we interpolated the missing or abnormal data from a few sites using the mean value of the data from adjacent sites in the same period. Furthermore, the seasonal differences in surface humidity and natural vegetation distribution in the study area were compared and analyzed by dividing the time series into four seasons: spring (March, April and May), summer (June, July and August), autumn (September, October and November) and winter (December, January and February). It is worth noting that based on the latitudinal position of the Qinling-Huaihe Line and the feasibility of map operations, we defined the area north of 35°N as the northern China, i.e., the study area (Fig. 1), to reduce the error caused in statistical analyses based on administrative

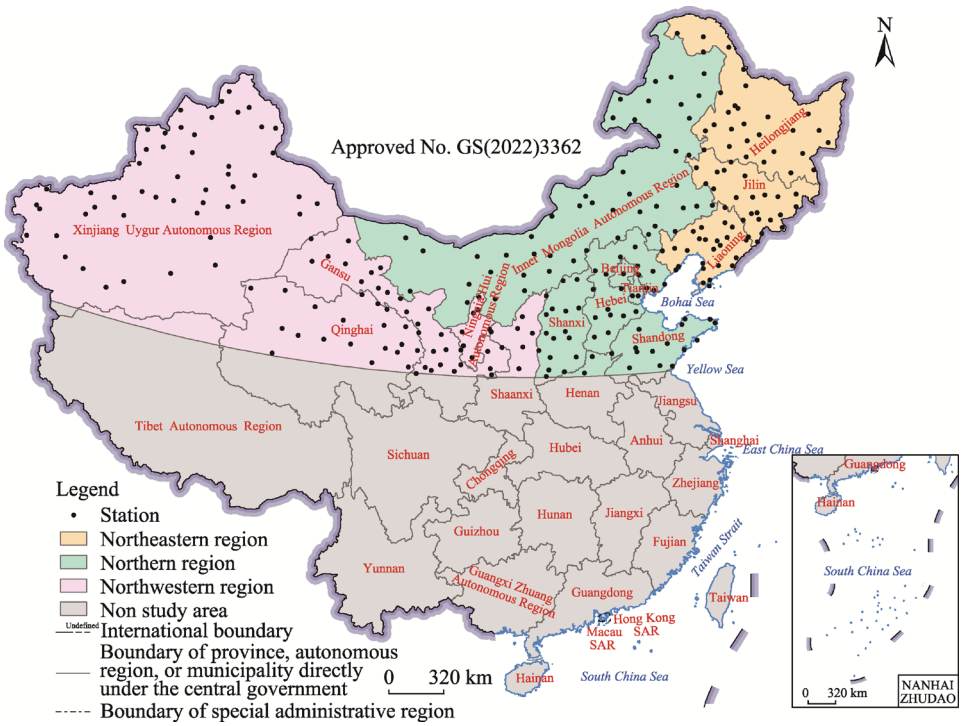

Fig. 1 Location of the study area (northern China) and spatial distribution of meteorological stations. SAR, special administrative region.

divisions. Therefore, the meteorological data and land use/land cover data from the provinces, autonomous regions and municipalities considered in this study represent the changes in north of 35°N in China.

The surface wetness index (SWI) is an important indicator used to measure the dry-wet condition of regional surfaces; it characterizes the income and expenditure of water at different spatial and temporal scales according to the relationship between precipitation and evapotranspiration (Hulme et al., 1992; Luo et al., 2016; Han et al., 2019). Based on the existing research and considering the influence of regional climate conditions on the accuracy of the reanalysis method, we selected the Penman–Monteith formula that has the highest accuracy and clearest physical meaning in both arid and humid areas, to calculate potential evapotranspiration (Allen et al., 1989, 1998; Du et al., 2001; Mao et al., 2011). The Penman–Monteith formula is also the only standard method recommended by the Food and Agriculture Organization of the United Nations (FAO) for calculating potential evapotranspiration. The calculation process is as follows:

$$\mathrm{ET}_0 = \frac{0.408\Delta(R_n - G) + \gamma \frac{900}{T + 273} u_2 (e_s - e_a)}{\Delta + \gamma(1 + 0.34u_2)}, \tag{1}$$

$$\mathrm{SWI} = \mathrm{P} / \mathrm{ET}_0, \tag{2}$$

where ET_0 is the potential evapotranspiration (mm/d); R_n is the net surface radiation of crops (MJ/(m^2·d)); G is the soil heat flux (MJ/(m^2·d)), which is approximately zero when calculating the daily potential evapotranspiration; γ is a wet-dry constant obtained from a table (kPa/°C); T is the average temperature at a height of 2.0 m (°C); u_2 is the wind speed at a height of 2.0 m (m/s); e_s is the saturated vapour pressure (kPa); e_a is the actual water vapour pressure (kPa); Δ is the slope of the saturated vapour pressure curve (kPa/°C); SWI is the surface wetness index; and P is the precipitation (mm/d). The larger the SWI value is, the more humid the surface, and vice versa.

In research on the impact of LUCC on climate, some scholars have proposed the "observation minus reanalysis" method (Kalnay and Cai, 2003). According to this method, we defined the atmospheric relative humidity (ARH) data observed at 1.5 m above the ground recommended by the National Meteorological Research Center as the observed humidity values and the SWI as the reanalysis humidity value. In the process of calculating the SWI, both a series of influencing factors of the ARH and the underlying surface were involved. Therefore, it is necessary to use the principle of the reanalysis minus observation (RMO) method to subtract the observed humidity (i.e., ARH) from the reanalysis humidity (i.e., SWI) in the study area; in this way, the difference of surface humidity (i.e., RMO) can be obtained, and the spatial heterogeneity of surface humidity caused by differences in the physical and chemical properties of the underlying surface can be fully considered. The RMO can effectively characterize the impact of different land use/land cover types on surface humidity. Therefore, we selected the RMO to characterize the surface humidity at 1.5 m above the ground. The calculation process is as follows:

$$\mathrm{RMO} = \mathrm{SWI} - \mathrm{ARH}, \tag{3}$$

where ARH is the atmospheric relative humidity observed at 1.5 m above the ground recommended by the National Meteorological Research Center (%) and RMO is the difference between the SWI and ARH (%), which is mainly used to characterize the surface humidity.

Since the slope of the linear trend can characterize the change trend of different indicators, we fitted the RMO values of 292 meteorological stations in the study area during the period of 1991–2018 using univariate linear regression, and obtained the change trend of the RMO. The corresponding formula used to calculate the change trend is as follows:

$$\mathrm{Slope} = \frac{n\sum_{i=1}^{n} i x_i - \sum_{i=1}^{n} i \sum_{i=1}^{n} x_i}{n\sum_{i=1}^{n} i^2 - \left(\sum_{i=1}^{n} i\right)^2}, \tag{4}$$

where slope is the slope degree of the RMO linear fitting; n is the time series; i is the year; and x_i is the RMO value in year i. The value of slope higher than zero means that the RMO is increasing, while the value of slope lower than zero means that the RMO is decreasing.

2.3 Land use/land cover data and processing

The MCD12Q1 remote sensing image data used in this study were provided by the Google Earth Engine (GEE) platform with a spatial resolution of 500 m. The image data were preprocessed and interpreted by ENVI 5.3 and ArcGIS 10.2, and the main processing steps included band combination, reclassification, image clipping and confusion matrix accuracy verification (Jing et al., 2017). On the basis of the International Geosphere-Biosphere Programme (IGBP) classification, we divided the land use/land cover types in the study area into six categories: forestland, grassland, cultivated land, construction land, water body and unused land (bare surface such as desert and Gobi) by using the method of combining supervised classification with visual interpretation classification and referring to the land use classification method of the Chinese Academy of Sciences (Liu et al., 2010, 2014). Finally, based on the GEE platform, we used the confusion matrix method to evaluate the accuracy of land use/land cover data in 2001, 2010 and 2018 (Dai et al., 2021). The overall classification accuracies of the land use/land cover data in 2001, 2010 and 2018 were 98.54%, 98.68% and 97.83%, respectively, and the corresponding Kappa coefficients were 0.969, 0.972 and 0.955, respectively, which satisfy the accuracy requirements of this study.

The land use/land cover transfer matrix represents an application of the Markov model in LUCC, and this method can comprehensively and specifically describe the quantity and dynamics of mutual transfer of different land use/land cover types in a region. This matrix is derived from a quantitative description of the system state and state transfer in the system analysis. In this paper, we calculated the transfer matrix of various land use/land cover types in each period through the ENVI supervised classification method to obtain the change and transfer area of different land use/land cover types. Then, we introduced the area growth index to explore the changes in different land use/land cover types and their influence on surface humidity in the study area. Finally, combined with the expansion and reduction of land use/land cover types in different regions, we made a simple judgement on the future trend of regional surface humidity:

$$N_c = \frac{A_i^{t+1} - A_i^t}{A_i^t} \times 100\%, \tag{5}$$

where N_c is the area growth index (%); A_i^{t+1} is the area of the i^{th} land use/land cover type in period t+1 (km^2); and A_i^t is the area of the i^{th} land use/land cover type in period t (km^2) (Jing et al., 2017).

3 Results

3.1 Relationship between LUCC and surface humidity

3.1.1 Time series characteristics of surface humidity

The temporal variations of the ARH and SWI in the study area from 1991 to 2018 are shown in Figure 2a. This comparison shows that the ARH in northern China declined slightly but maintained stable during the study period, and the ARH generally exhibited a slight drying trend in the study area. The SWI, however, showed obvious fluctuation characteristics; specifically, before 2000, the fluctuation trend of the SWI was mainly downwards, with a small fluctuation range, while after 2000, the fluctuation range of the SWI was larger and the upwards trend was obvious. Therefore, it could be concluded that the variation trend of the SWI was not consistent with that of the ARH, and the difference between them could be attributed to the interference of the underlying surface influencing factors on the SWI being much stronger than that on the ARH.

Combined with Figure 2b, the variation trend of the RMO in the study area was highly consistent with that of the SWI. The RMO also showed a trend of first decreasing and then increasing during the period of 1991–2018, with the year 2000 as the inflection point. The

fluctuation trends of both were almost synchronous. Accordingly, from 1991 to 2018, the surface of northern China showed a trend of drying first and then wetting, and the degree of wetness in the later period was much higher than that in the earlier period. In general, under the background of the downwards trend of the ARH, the surface of northern China became wetter during the study period (1991–2018). After the beginning of the 21st century, regional surface humidification was particularly obvious, which may be related to the impact of LUCC.

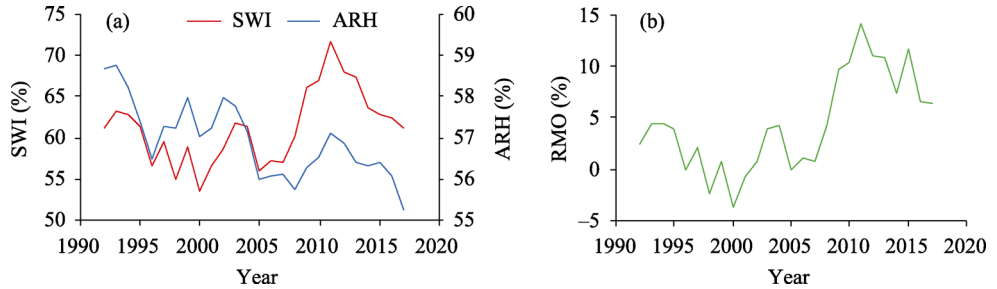

Fig. 2 Moving average time series of the SWI and ARH (a) and RMO (b) from 1991 to 2018 in northern China. SWI, surface wetness index; ARH, atmospheric relative humidity; RMO, reanalysis minus observation.

3.1.2 Contributions of different land use/land cover types to surface humidity

The land use/land cover types exhibited significant regional differences in terms of the RMO values due to their unique physical and chemical properties. In the areas with poor land cover, the land surface was mostly exposed and the moisture in the topsoil was easy to lose due to the direct influence of wind and solar radiation and other factors. Thus, surface humidity in these areas was low. Conversely, in well-covered areas, most vegetation had a protective effect on the land surface. At the same time, due to the water retention and water holding characteristics of vegetation, surface water was not easy to lose directly. In addition, plant evapotranspiration could increase the local ARH and promote the regional water cycle to a certain extent, ultimately increasing surface humidity. To highlight the sensitivity of the difference among the RMO values to land use/land cover types, we adopted the divisional statistical tool to determine the contributions of different land use/land cover types to the regional RMO in northern China in the 21st century (Fig. 3).

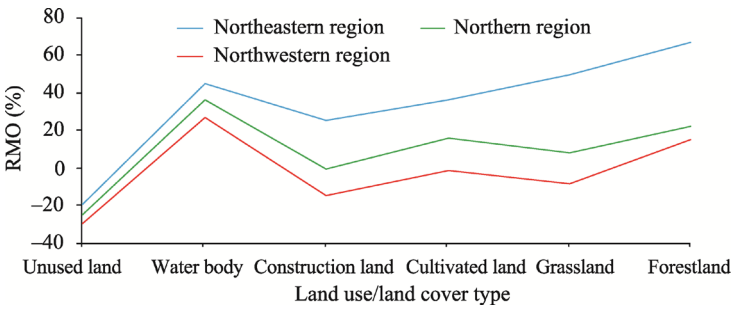

Fig. 3 Average RMO values for different land use/land cover types in different regions of northern China during the period of 2001–2018

From the perspective of the entire study area, the contributions of different land use/land cover types to the RMO had remarkable differences in the same region. Forestland and water body had the most positive contributions to the RMO. However, unused land and construction land had the most negative contributions to the RMO. In view of the different partitions, due to the different geographical environments, the regional differences for the same land use/land cover type were exceedingly obvious. Among them, forestland in northeastern region had the largest positive contribution to the RMO (66.54%), followed by that in northern region (21.93%) and northwestern region (15.20%). Similarly, water body, which made a large positive contribution to the RMO, also showed the characteristic of decreasing gradually from northeast to northwest.

Nevertheless, the negative contribution of unused land to the RMO was the lowest in northeastern region (–19.63%), followed by northern region (–24.81%) and northwestern region (–29.80%). Because of the strong influence of human activities, the negative contribution of construction land to the RMO was also large. In northern region and northwestern region, the negative contributions of construction land were –0.72% and –14.82%, respectively. It is worth noting that the RMO contribution from different land use/land cover types was the highest in northeastern region and the lowest in northwestern region. Except for unused land, the other land use/land cover types in northeastern region all featured positive contributions to the RMO. In northwestern region, except for water body and forestland, the other land use/land cover types displayed different degrees of negative contributions to the RMO.

In summary, the contribution of the same land use/land cover type to the RMO varied under different ecological environments. For example, in northeastern region, where the ecological environment was better, the contribution of forestland was obviously greater than that in northwestern region, where the ecological environment was fragile. Similarly, the obvious negative contribution of unused land to the RMO was far lower in northeastern region than in northwestern region, indicating that the impact of LUCC on surface humidity was related to the regional ecological environmental quality.

3.2 Impact of LUCC on surface humidity

3.2.1 Spatial variation characteristics of land use/land cover types

The combination of the spatial distribution of LUCC in northern China in the 21st century (Fig. 4) and the statistical areas of LUCC in the study area in the same period (Table 1) reveals that the shrinkage of grassland in northeastern region was serious, decreasing by approximately 1.04×10^4 km^2 from 2001 to 2018. The main degradation areas were concentrated in northern Heilongjiang and southeastern Liaoning. The remaining land use/land cover types showed various degrees of expansion. Specifically, forestland expanded by 0.67×10^4 km^2 and was mainly concentrated in the eastern and central forestland of northeastern region. In northern region, the areas of forestland, cultivated land and construction land also expanded to various degrees, with increases of 1.10×10^4, 0.95×10^4 and 0.41×10^4 km^2, respectively. The areas of the other three remaining land use/land cover types decreased, with the area of unused land decreasing the most (1.53×10^4 km^2), followed by grassland (0.90×10^4 km^2). In addition, in northwestern region, except for the considerable reduction of unused land (decreasing by approximately 3.70×10^4 km^2), the remaining land use/land cover types displayed different degrees of expansion, with the area of cultivated land expanding by approximately 2.23×10^4 km^2 and the area of grassland expanding by approximately 1.36×10^4 km^2. In conclusion, the ecological environment in northern China was improved in the study area, with the coverage of forestland expanding (increasing by approximately 1.80×10^4 km^2) and the coverage of unused land reducing (decreasing by approximately 5.15×10^4 km^2).

3.2.2 Sensitivity of spatial variations in the RMO to LUCC

The changes in the areas of different land use/land cover types across northern China in the 21st century were obtained using the transfer matrix (Table 2). The spatial distribution of LUCC (Fig. 4) and the changes in the RMO trend values (Fig. 5) demonstrated a good correlation between them. In northeastern region, the areas of forestland and water body expanded with the largest positive contributions to the RMO, and the RMO trend was relatively large, with the most rapid growth rate of 0.34/10a. In northern region, especially in western Inner Mongolia and western Shanxi, where the areas of forestland and grassland expanded and the area of unused land reduced, the RMO showed an increasing trend, while the RMO in most other areas showed an overall decreasing trend because of the obvious negative contributions of unused land and construction land. Similarly, in northwestern region that was dominated by the reduction of unused land area accompanied by different degrees of expansion of forestland, grassland and water body, the RMO exhibited an increasing trend, and the surface of the region tended to become wetter. In some areas in which construction land and cultivated land expanded, such as

Gansu, Ningxia and Shanxi, the RMO trend value was the smallest (the minimum value of 0.89/10a), and the drying trend of the land surface was the strongest. In general, in the 21st century, surface humidity in northern China mainly exhibited weak humidification. The change in surface humidity was closely related to the variation in regional vegetation coverage; when the regional vegetation coverage with positive (negative) contributions expanded (reduced), the land surface became wetter.

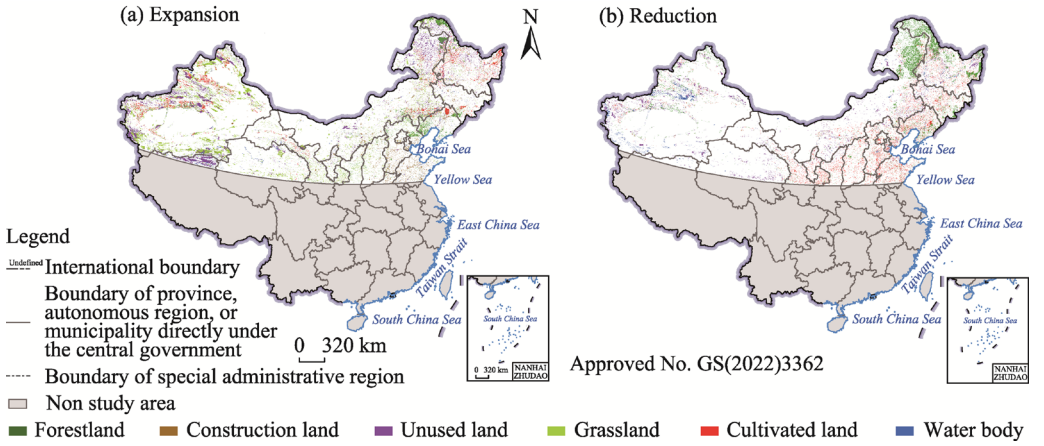

Fig. 4 Spatial distribution of land use/land cover change (LUCC) in northern China during the period of 2001–2018. (a), expansion of land use /land cover types; (b), reduction of land use /land cover types. Blank areas in northern China are the areas with no change in land use /land cover types.

Table 1 Area changes for different land use/land cover types in northern China during the period of 2001–2018

Region	Change in area ($\times 10^4$ km^2)					
	Forestland	Grassland	Construction land	Cultivated land	Water body	Unused land
Northeastern region	0.67	–1.04	0.14	0.09	0.06	0.08
Northern region	1.10	–0.90	0.95	0.41	–0.02	–1.53
Northwestern region	0.03	1.36	2.23	0.01	0.08	–3.70

Note: The positive value indicates the area expansion, while the negative value indicates the area reduction.

Table 2 Area growth index values for different land use/land cover types in different regions of northern China during the period of 2001–2018

Region	Province/Autonomous region/Municipality	Area growth index (%)					
		Forestland	Grassland	Cultivated land	Construction land	Water body	Unused land
Northeastern region	Heilongjiang	5.58	–9.41	1.86	6.96	18.70	69.47
	Jilin	1.73	–16.19	6.20	11.00	34.40	47.30
	Liaoning	2.73	12.98	–8.58	13.89	0.98	25.16
Northern region	Inner Mongolia	15.90	0.41	16.44	5.64	–12.45	–6.42
	Beijing and Tianjin	–2.33	9.72	–12.64	13.13	4.89	21.42
	Hebei	20.53	2.77	–5.49	17.23	0.78	63.22
	Shandong	71.49	7.70	–2.82	20.87	1.16	38.05
	Shanxi	61.62	–15.89	35.63	6.17	39.67	16.29
Northwestern region	Shaanxi	2.39	–1.67	8.63	6.63	–16.55	–50.38
	Gansu	19.99	2.32	17.12	1.43	18.59	–4.83
	Ningxia	129.02	–2.58	21.69	17.85	–11.11	–61.37
	Qinghai	38.49	4.94	–13.17	1.52	9.89	–3.46
	Xinjiang	–17.40	3.10	55.69	0.58	7.34	–3.09

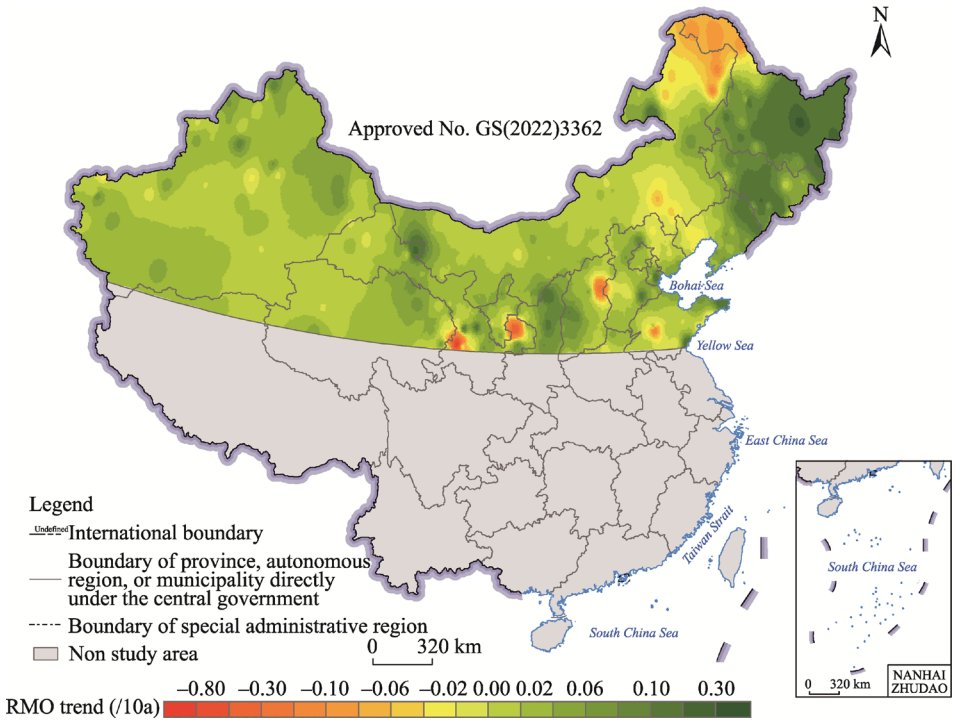

Fig. 5 Spatial pattern of the RMO trend changes in northern China during the period of 2001–2018

3.3 Sensitivity comparison of the seasonal RMO changes to land use/land cover types

Northern China is located north of the Qinling-Huaihe Line where the temperature changes clearly in the four seasons (the average temperature being lower than 0°C in January) and the surface coverage varies significantly. Based on these characteristics, it is necessary to explore the variation in the RMO in different seasons in northern China.

The spatial correlation between the RMO values in the four seasons (Fig. 6) and the natural vegetation distribution (Fig. 7) was analyzed and compared. The seasonal variation in the RMO values in northern China was closely related to the distribution of natural vegetation. In general, the RMO values decreased gradually from east to west in different seasons in the study area, which was in good correspondence with the pattern of more natural vegetation distributed in the east and less natural vegetation distributed in the west. Among them, the RMO values of the whole study area was low in spring, and the range of high values was not large, mainly distributed in northeast region where forestland is concentrated. In summer, the RMO values increased significantly, and the range of high values expanded from forestland in northeastern region to grassland in northern region and the eastern part of northwestern region. In autumn, the RMO values in the study area showed a decreasing trend, and the range of high values began to reduce compared with those in summer. In winter, the range of the high RMO values concentrated in forestland of northeastern region. At the same time, land surfaces of northern region and northwestern region entered an abnormal drought period. It is worth mentioning that in northern China, the low value centers of the RMO in the four seasons were always concentrated in unused land.

4 Discussion

The transformation of land use/land cover types is a dynamic process, and LUCC is the product of this process. With the rapid development of social economy, human beings are continuously reshaping the land surface of the Earth, and the area is getting bigger and bigger, which has changed the land use/land cover types and vegetation coverage to some extent. It is generally

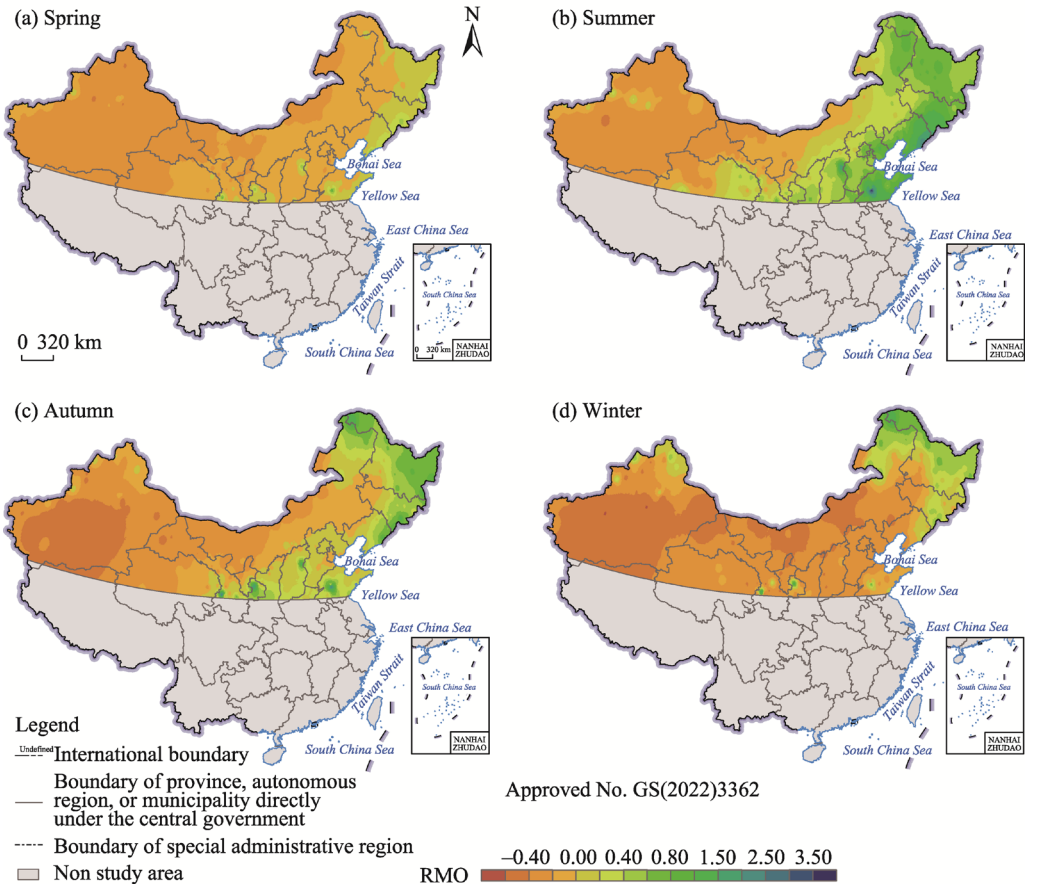

Fig. 6 Spatial distribution of the RMO in spring (a), summer (b), autumn (c) and winter (d) in northern China during the period of 2001–2018

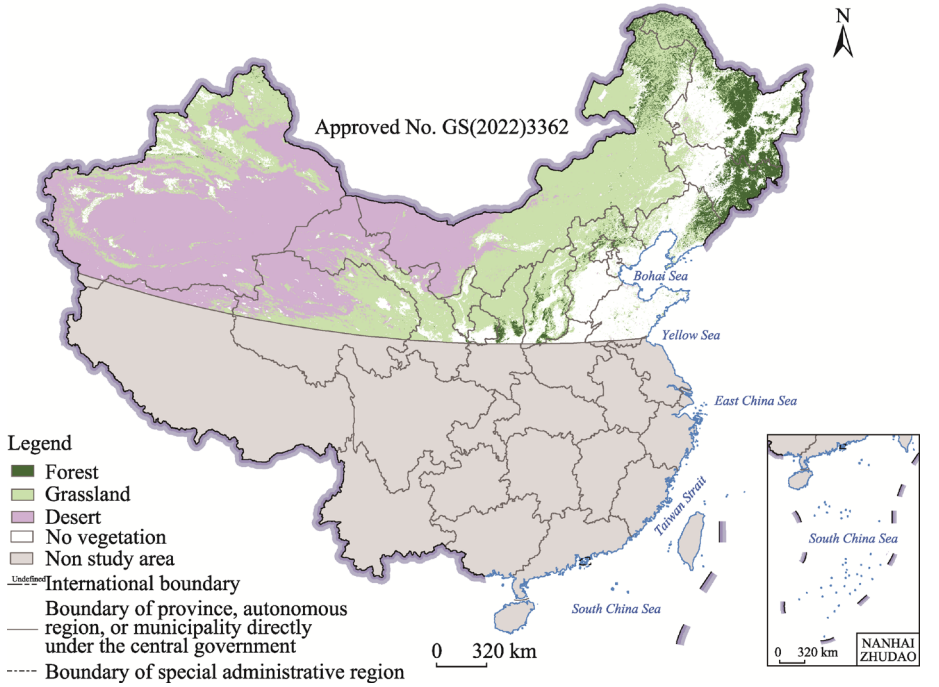

Fig. 7 Spatial distribution of natural vegetation in northern China during the period of 2001–2018

known that China is one of the regions with the highest intensities of human activities in the world due to its complex terrain and diverse underlying surface types, therefore, it is also one of the most representative research areas of LUCC (Hua et al., 2014). Similarly, northern China not only spans a large area but also features complex and diverse terrain, so the east–west climate difference is obvious. Thus, affected by the uneven distributions of regional water and heat, the LUCC in each region presents the characteristics of synchronous expansion and reduction, and the ranges of change are quite different.

LUCC is one of the most important ways that human activities affect the Earth's climate. According to the report of the National Research Council (2005), the contribution of LUCC to climate change will even exceed the contribution of greenhouse gases. In the end of the 20th century, Chinese governments have implemented ecological protection projects to improve the ecological environment, control soil and water loss and prevent wind and sand hazards in northern China (Zhang et al., 2009; Mao et al., 2017). Affected by these efforts, the land cover situation in northern China has changed greatly. On the one hand, the climate effect of global warming with increasing emissions of greenhouse gases has been widely noted. On the other hand, compared with humidity data, temperature data have the advantages of more extensive, easier to collect, longer time series, good continuity, etc. Therefore, studies on the impact of LUCC on the regional climate have mainly concentrated on temperature, whereas research on the regional degrees of dryness and wetness is relatively limited. Kaufmann et al. (2007) studied the impact of urbanization on precipitation in the Pearl River Delta and found that rapid urbanization has led to a reduction in regional precipitation. Similarly, studies have shown that since the 1980s, rapid urbanization in Beijing has been closely related to the decrease in local summer precipitation (e.g., Zhang et al., 2009). In addition, other studies suggest that urbanization has led to a decline in relative humidity in urban areas and a slight increase in relative humidity in suburban areas (Li et al., 2008; Zheng and Liu, 2008; Zhao et al., 2011). There is no doubt that the pattern of LUCC affects the local climate. Therefore, understanding the change trends of land use/land cover types allows us to not only assess human activities on land use types but also judge the direction in which land use/land cover types are changing to predict the development trend of regional surface humidity. It could be inferred from the transfer matrix (Table 2) that surface humidity in northeastern region will increase in the future, but it is necessary to pay attention to the protection of regional ecology and prevent the continuous expansion of unused land. Similarly, the RMO in northern region will decline in the future, and land surface here will tend to become drier; therefore, it should pay attention to control the expansion of construction land strictly. At the same time, in urban planning, the construction of artificial wetlands (artificial lakes, wetland parks, etc.) and forest parks and other humidification projects could be appropriately increased to improve the surface humidity and promote the suitability of the living environment to a certain extent. Finally, the RMO values in northwestern region may increase in the future, and land surface will become wetter. This region should continue to strengthen the governance of the vast desert areas and improve the quality of the regional ecological environment.

Through the above analysis, it was found that the seasonal variation in the RMO values in northern China had a strong response to the growth of regional natural vegetation. In winter and spring, due to the limitation of climatic conditions, plant species in grassland could not grow normally, then the grasses dried out and the leaves withered. The original green vegetation basically lost the ability to retain water. Therefore, the physical and chemical properties of the underlying surface of grassland were similar with those of unused land, and surface water was easy to be lost directly. Therefore, in winter and spring, the land surface of most areas in northern China was dry except for that in forestland of northeastern region. The degree and range of surface drying in winter were much larger than those in spring. In contrast, the climatic factors in summer and autumn were very beneficial to the growth of regional natural vegetation. Especially in summer, the vegetation coverage in most areas of northern China reached the maximum for the year. On the one hand, the expansion of vegetation-covered area was conducive to the maximum absorption and retention of surface water by the vegetation, so surface water was not easy to be lost directly. On the other hand, the expansion of vegetation-covered area promoted the regional

hydrological cycle to a certain extent, so the regional ecological environment presented a constructive cycle and further played a role in humidifying the regional land surface.

In conclusion, the ARH in northern China declined slightly but maintained stable during the study period, and the ARH generally exhibited a slight drying trend in the study area. This conclusion agrees with previous research results (Wang and Zhang, 2008; Bian et al., 2011; Yao et al., 2017). Under this climate background, we chose northern China as an example to analyze the change trends of regional land use/land cover types and surface humidity, and it was found that the feedback effect of land use/land cover types on surface humidity exhibits an obvious spatial heterogeneity. Finally, we assessed the change trends of surface humidity in different regions of northern China, and the conclusions are basically consistent with those of previous studies (Bian et al., 2013; Yuan et al., 2017; Jia and Zhang, 2019). However, by referring to previous research theories (Kalnay and Cai, 2003), we used the RMO method to simply obtain the surface humidity from the SWI; nevertheless, further analysis of the internal mechanisms and factors that strongly influence the two types of humidity is lacking. In the future, we should strengthen the positioning and research of the relevant data, carry out more numerical experiments and analysis, and distinguish the impact of LUCC on climate more accurately.

5 Conclusions

In recent years, the land surface in northern China has become wetter in general. The RMO values for different land use/land cover types featured significant regional differences due to their unique physical and chemical properties. In general, the change in surface humidity was closely related to the variation in regional vegetation coverage; when the regional vegetation coverage with positive (negative) contributions expanded (reduced), the land surface became wetter. In addition, the seasonal variation of regional surface humidity was closely related to the vegetation growth in different seasons under the influence of special climatic conditions in the study area. It can be inferred that surface humidity in both northeastern region and northwestern region of northern China will increase in the future, but the surface will tend to be drier in northern region. Thus, special attention should be paid to the rational planning of land use/land cover types to improve the quality of the regional ecological environment. On this basis, we will work on future studies to explore the planning status and problems of land use/land cover types in different regions and propose practical suggestions for the sustainable development of the regional ecological environment from the perspective of ecological restoration.

Acknowledgements

This study was funded by the National Natural Science Foundation of China (42071112, 41771110). We thank the editors and anonymous reviewers whose insights and suggestions have greatly improved this manuscript.

References

Allen R G, Jensen M E, Wright J L, et al. 1989. Operational estimates of reference evapotranspiration. Agronomy Journal, 81(4): 650–662.

Allen R G, Pereira L S, Raes D, et al. 1998. Crop evapotranspiration: guidelines for computing crop water requirements. Fao Irrigation and Drainage Paper 56. Rome: Food and Agriculture Organization of the United Nations.

Bian J C, Chen H B, Vömel H, et al. 2011. Intercomparison of humidity and temperature sensors: GTS1, Vaisala RS80, and CFH. Advances in Atmospheric Sciences, 28(1): 139–146.

Bian J J, Hao Z X, Zheng J Y, et al. 2013. The shift on boundary of climate regionalization in China from 1951 to 2010. Geographical Research, 32(7): 1179–1187. (in Chinese)

Bian X H, Liu Y, Ding Q Q, et al. 2019. Response of land use and cover change to urban heat island effect in Huzhou City, Zhejiang Province. Bulletin of Soil and Water Conservation, 39(3): 263–269. (in Chinese)

Braswell B H, Schimel D S, Linder E, et al. 1997. The response of global terrestrial ecosystems to interannual temperature variability. Science, 278(5339): 870–873.

Buitenwerf R, Rose L, Higgins S I. 2015. Three decades of multi-dimensional change in global leaf phenology. Nature Climate

Change, 5(4): 364–368.
Cao L J, Zhang D F, Zhang Y, et al. 2010. Sensitivity research of the effects of land use change on climate and runoff over the Yangtze River basin. Chinese Journal of Atmospheric Sciences, 34(4): 726–736. (in Chinese)
Dai X Q, Shen R Q, Wang J, et al. 2021. Change detection of land use in Henan Province based on GEE remote sensing cloud platform. Journal of Geomatics Science and Technology, 38(3): 287–294.
Du Y D, Liu Z X, Zhang Y F. 2001. Evaluaiton of two reference crop evapotranspiration calculation methods. Journal of Henan Agricultural University, 35(1): 57–61. (in Chinese)
Dumont B, Andueza D, Niderkorn V, et al. 2015. A meta–analysis of climate change effects on forage quality in grasslands: specificities of mountain and M editerranean area. Grass and Forage Science, 70(2): 239–254.
Fezzi C, Harwood A R, Lovett A A, et al. 2015. The environmental impact of climate change adaptation on land use and water quality. Nature Climate Change, 5(3): 255–260.
Fu B J, Yu D D, Lü N. 2017. An indicator system for biodiversity and ecosystem services evaluation in China. Acta Ecologica Sinica, 37(2): 341–348. (in Chinese)
Gao J B, Jiao K W, Wu S H. 2019. Investigating the spatially heterogeneous relationships between climate factors and NDVI in China during 1982 to 2013. Journal of Geographical Sciences, 29(10): 1597–1609.
Han H Q, Zhang C Q, Wang Y, et al. 2019. Spatial-temporal variation and influencing factors of dry and wet condition in Guizhou Province between 1961 and 2014. Journal of Shanxi Agricultural University (Nature Science Edition), 39(4): 106–112. (in Chinese)
Hua W J, Chen H S, Li X. 2014. Review of land use and land cover change in China and associated climatic effects. Advances in Earth Science, 29(9): 1025–1036. (in Chinese)
Hulme M, Marsh R, Jones P D. 1992. Global changes in a humidity index between 1931–1960 and 1961–1990. Climate Research, 2: 1–22.
Hurtt G C, Chini L P, Frolking S, et al. 2011. Harmonization of land-use scenarios for the period 1500–2100: 600 years of global gridded annual land-use transitions, wood harvest, and resulting secondary lands. Climatic Change, 109(1–2): 117–161.
IPCC. 2019. Climate Change and Land: An IPCC special report on climate change, desertification, land degradation, sustainable land management, food security, and greenhouse gas fluxes in terrestrial ecosystems. Shukla P R, Skea J, Calvo Buendia E, et al. (eds.). [2021-08-12]. https://spiral.imperial.ac.uk/handle/10044/1/76618.
Jia Y Q, Zhang B. 2019. Relationship of dry-wet climate changes in Northern China in the past 57 years with Pacific Decadal Oscillation (PDO). Acta Pedologica Sinica, 56(5): 1085–1097. (in Chinese)
Jing Y Q, Zhang F, Chen L H, et al. 2017. Investigation on eco-environmental effects of land use/cover-landscape pattern and climate change in Ebinur Lake Wetland Nature Reserve. Acta Scientiae Circumstantiae, 37(9): 3590–3601. (in Chinese)
Kalnay E, Cai M. 2003. Impact of urbanization and land-use change on climate. Nature, 423: 528–531.
Kaufmann R K, Seto K C, Schneider A, et al. 2007. Climate response to rapid urban growth: Evidence of a human-induced precipitation deficit. Journal of Climate, 20: 2299–2306.
Lai L, Huang X, Yang H, et al. 2016. Carbon emissions from land-use change and management in China between 1990 and 2010. Science Advances, 2(11): e1601063, doi: 10.1126/sciadv.1601063.
Li S Y, Chen H B, Li W. 2008. The impact of urbanization on city climate of Beijing region. Plateau Meteorology, 27(5): 1102–1110. (in Chinese)
Li S Y, Liu X P, Li X, et al. 2017. Simulation model of land use dynamics and application: progress and prospects. Journal of Remote Sensing, 21(3): 329–340. (in Chinese)
Lin L, Fan H, Jin Y. 2020. Multi-scale and multi-model simulation of land use/land cover change in the mountainous county: A case study of Mengla County in Yunnan Province, China. Mountain Research, 38(4): 630–642. (in Chinese)
Liu J Y, Zhang Z X, Xu X L, et al. 2010. Spatial patterns and driving forces of land use change in China during the early 21st century. Journal of Geographical Sciences, 20(4): 483–494.
Liu J Y, Kuang W H, Zhang Z X, et al. 2014. Spatiotemporal characteristics, patterns and causes of land use changes in China since the late 1980s. Acta Geographica Sinica, 69(1): 3–14. (in Chinese)
Luo Q H, Ning H S, Chen Q M. 2016. Trends of surface dry-wet state of Ganjiahu in Xinjiang based on humid index. Arid Zone Research, 33(5): 921–926. (in Chinese)
Mao F, Sun H, Yang H L. 2011. Research progress in dry/wet climate zoning. Progress in Geography, 30(1): 17–26. (in Chinese)
Mao R X, Chen G, Zhang S Q. 2017. Several problems in the construction of the Three-North Shelter Forest Program and suggestions for its countermeasures. Protection Forest Science and Technology, (10): 58–59, 61. (in Chinese)
Mooney H A, Duraiappah A, Larigauderie A. 2013. Evolution of natural and social science interactions in global change

research programs. Proceedings of the National Academy of Sciences of the United States of America, 110(Suppl 1): 3665–3672.

National Research Council. 2005. Radiative Forcing of Climate Change: Expanding the Concept and Addressing Uncertainties. Washington D.C.: National Academies Press, 1–208.

Oleson K, Bonan G Feddema J, et al. 2008. An urban parameterization for a global climate model. Part I: Formulation and evaluation for two cities. Journal of Applied Meteorology and Climatology, 47(4): 1038–1060.

Pitman A J, Noblet-Ducoudé N, Cruz F T, et al. 2009. Uncertainties in climate responses to past land cover change: First results from the LUCID intercomparison study. Geophysical Research Letters, 36(14): L14814, doi: 10.1029/2009GL039076.

Shao P, Zeng X D. 2012. Progress in the study of the effects of land use and land cover change on the climate system. Climatic and Environmental Research, 17(1): 103–111. (in Chinese)

Sterling S M, Ducharne A, Polcher J. 2012. The impact of global land-cover change on the terrestrial water cycle. Nature Climate Change, 3(4): 385–390.

Sun L, Wu G X, Sun S F. 2000. Numerical simulations of effects of land surface processes on climate implementing of SSiB in IAP/LASG AGCM L9R15 and its performance. Acta Meteorologica Sinica, 58(2): 179–193. (in Chinese)

Sun Q, Qi W, Yu X Y. 2021. Impacts of land use change on ecosystem services in the intensive agricultural area of North China based on Multi–scenario analysis. Alexandria Engineering Journal, 60(1): 1703–1716.

Tian H Q, Chen G, Zhang C, et al. 2012. Century-scale response of ecosystem carbon storage to multifactorial global change in the Southern United States. Ecosystems, 15: 674–694.

Tuffour-Mills D, Antwi-Agyei P, Addo-Fordjour P. 2020. Trends and drivers of land cover changes in a tropical urban forest in Ghana. Trees, Forests and People, 2, doi: 10.1016/j. tfp. 2020.100040.

Verbeeck H, Kearsley E. 2015. The importance of including lianas in global vegetation models. Proceedings of the National Academy of Sciences of the United States of America, 113(1): E4, doi: 10.1073/pnas.1521343113.

Wang J H, Zhang L Y. 2008. Systematic errors in global radiosonde precipitable water data from comparisons with ground-based GPS measurements. Journal of Climate, 21(10): 2218–2238.

Wang M N, Ha Z, Zhang Q Y. 2016. Impact of land use and cover change in the semi-arid regions of China on the temperature in the early 21st century. Climatic and Environmental Research, 21(1): 65–77. (in Chinese)

Wang Q, Zhang Q P, Zhou W. 2012. Grassland coverage changes and analysis of the driving forces in Maqu County. Physics Procedia, 33: 1292–1297.

Wang X L, Liu Y, Zhang Y, et al. 2021. Exploration and prediction of land use/cover change in western Jilin province based on Ca-markov model. Science Technology and Engineering, 21(19): 7942–7948. (in Chinese)

Weinert M, Mathis M, Kröncke I, et al. 2016. Modelling climate change effects on benthos: Distributional shifts in the North Sea from 2001 to 2099. Estuarine, Coastal and Shelf Science, 175(20): 157–168.

Yang X C, Zhang Y L, Liu L S, et al. 2009. Sensitivity of surface air temperature change to land types in China. Science in China Series D-Earth Sciences, 52(8): 1207–1215.

Yao W, Ma Y, Gao L N. 2017. Comparison of relative humidity data between L-band and 59-701 sounding system. Journal of Applied Meteorological Science, 28(2): 218–226. (in Chinese)

Yuan Q Z, Wu S H, Dai E F, et al. 2017. Spatio-temporal variation of the wet-dry conditions from 1961–2015 in China. Science China: Earth Sciences, 47(11): 1339–1348.

Zhang C L, Chen F, Miao S G, et al. 2009. Impacts of urban expansion and future green planting on summer precipitation in the Beijing metropolitan area. Journal of Geophysical Research, 114: D02116, doi: 10.1029/2008JD010328.

Zhang X R, Song W, Lang Y Q, et al. 2020. Land use changes in the coastal zone of China's Hebei Province and the corresponding impacts on habitat quality. Land Use Policy, 99, doi: 10.1016/j.landusepol.2020.104957.

Zhang Z X, Liu L M, Jia Y, et al. 2009. Climatic ecological adaptation of shelter forests in Three-North Regions. Chinese Journal of Ecology, 28(9): 1696–1701. (in Chinese)

Zhao N, Liu S H, Yu H Y. 2011. Urbanization effects on local climate in Beijing in recent 48 years. Chinese Journal of Atmospheric Sciences, 35(2): 373–385. (in Chinese)

Zheng S Y, Liu S H. 2008. Urbanization effect on climate in Beijing. Climate and Environmental Research, 13(2): 123–133. (in Chinese)